Journal of Indian Geomorphology
Volume 12, 2024 ● ISSN 2320-0731
Indian Institute of Geomorphologists (IGI)

Modelling Soil Erosion Risk in the Kumari River Basin, India: A Revised Universal Soil Loss Equation (RUSLE)-Based Empirical Approach

Md. Hasanur Jaman, Subha Roy, Jaya Chatterjee,
Souvik Das and Somasis Sengupta
Department of Geography, The University of Burdwan, Bardhaman, West Bengal – 713104
E-mail: ssengupta@geo.buruniv.ac.in (Corresponding Author)

Abstract: *In the current era of Anthropocene, soil erosion has emerged as a major natural hazard. This process has resulted into a rapid loss of fertile topsoil which has made the goal of agricultural sustainability a difficult one. Moreover, there is also an augmentation of the siltation of the rivers and dams as a result of increased sediment load in the rivers. This problem is very significant in a country like India where a significant proportion of the population is still dependent on agriculture. As the actual measurement of erosion is quite complex and time-consuming, the exercise of assessing the erosion risk in a region is mostly dependent on prediction-based models. One such model is the Revised Universal Soil Loss Equation (RUSLE) which gives a reasonably reliable estimate of the ongoing process of erosion. The present paper attempts to quantify the amount of soil loss occurring in the Kumari river basin of eastern India with the help of the empirical Revised Universal Soil Loss Equation (RUSLE) Model. It is observed that in the basin, several areas are associated with high soil loss (>30 ton ha^{-1} yr^{-1}), especially in the upland regions of Ajodhya and Dalma Ranges. Also, an attempt has been made to extract the sub-basin and village-wise soil loss in the basin. In the Totko-Jam sub-basin and its encompassed villages, the situation is of concern. Therefore, such villages need to be prioritised in any exercise of soil conservation. This approach is expected to be effective in a country like India where the availability of resources is often limited.*

Keywords: Soil erosion, RUSLE, Kumari, sub-basin prioritisation

Introduction

The process of soil erosion is influenced by several factors, operating in combination (Wischmeier and Smith, 1978; Renard *et al*., 1997; Mutua *et al*., 2006; Butt *et al*., 2010). In the global context, runoff is the most significant operating factor of soil erosion and degradation which is influenced by a host of physiographic and environmental determinants such as precipitation, soil characteristics, and slope (Dutta *et al*., 2017; Oliveira *et al*., 2019). However, many anthropogenic factors viz., agricultural practices, deforestation, and different constructional activities play a significant role in accelerating soil loss and degradation. Land use landcover (LULC) distribution also acts in modifying the pattern of action and

amount of soil loss in a watershed or any other areal unit. The rhythmic alteration in LULC is accompanied by the corresponding change in soil characteristics and runoff (Setegn *et al*., 2010; Gebremicael *et al*., 2013; Kim *et al*., 2013; Buendia *et al*., 2016). In many developing countries where agriculture is the prime occupation of a large proportion of the population, soil erosion becomes a highly influential quasi-natural hazard and adequate measures of soil management are an emergent exercise in this domain (Kim *et al*., 2005; Lim *et al*., 2005).

Among the various agents, running water emerges as the most crucial agent of soil erosion. At the global scale, about 36 billion tons of top soil is lost every year due to removal by water, which, in turn gets augmented by deforestation and corresponding anthropogenic alterations (Borrelli *et al*., 2017). Augmented erosion results into increasing the sediment load in the rivers and approximately 15±0.5 Giga tons of sediment load is reaching the oceans at a global scale (Zhu *et al*., 2021). The rates of potential soil erosion in about 91 % of the entire land area of the world range from <5 to 40 ton ha^{-1} yr^{-1}, therefore, the primary task of policymakers across the world is to ensure adequate management of soil erosion (Sharda *et al*., 2013). The exact quantification of erosion is unfeasible and also unviable which ensures that the prediction-based models are particularly popular in this domain. A large number of soil erosion and sediment transport models can be observed in different literature in a global context (Lorup and Styczen, 1996). These models are predominantly based on index and usually consider multiple parameters, selections which may vary depending on the study area, data availability, and the importance of each parameter (Hoyos, 2005; Lim *et al*., 2005; Yuksel *et al*., 2008; Yue-Qing *et al*., 2009). Among numerous soil erosion prediction models found in the literature, the Universal Soil Loss Equation (USLE) and the Revised Universal Soil Loss Equation (RUSLE) are well-known for predicting the annual soil erosion rates in different catchments varying in areal extent (Lee, 2004; Pandey *et al*., 2009; Prasannakumar *et al*., 2012). The RUSLE Model looks at five major factors namely rainfall (R), soil erosion (K), slope length and steepness (LS), crop management (C), and conservation practice (P) (Sheikh *et al*., 2011). These five factors contribute to the risk of erosion and act as both the physical (slope, rainfall, and pedology) and anthropogenic (earth, conservation processes, etc.) proxies (Prasannakumar *et al*., 2012; Farhan *et al*., 2013). At the field scale, the traditional RUSLE method was suitable, wherein, topographical maps and field-based techniques were employed to determine the conditional factors of RUSLE, but these methods are not applicable at the catchment scale. With the introduction of remote sensing (RS) and Geographical Information Systems (GIS), basins that are larger in areal extent could be analyzed in detail and predicted for annual soil losses (Lin *et al*., 2002; Wang *et al*., 2002; Jasrotia and Singh, 2006; Chou, 2010; Roy *et al*., 2022). In this paper, the annual soil loss occurring in the Kumari river Basin has been estimated with the help of the empirical RUSLE Model by amalgamating field and RS-GIS techniques.

The study area

The Kumari river basin, a significant sub-basin of the Kangsabati river in eastern India has been selected for the present study. The river rises from the Bagmundi Upland near

Muadi Reserve Forest of the Ajodhya Hilly Region and flows WNE to ESE direction and ultimately debouches into the Kangsabati river at Mukutmanipur reservoir. The total area of the basin is 2002.62 km^2 and is subdivided into 36 sub-basins wherein the area of the sub-basin ranges from below 10 km^2 to above 500 km^2. The basin is located largely in the Purulia district of West Bengal except for a small part that lies in the neighboring state of Jharkhand, demarcated by 22°42′23″ N to 23°12′36″ N latitudes and 86°42′36″ E to 86°48′24″ E longitudes. Administratively, the basin is divided into 14 Community Development Blocks that hold 942 villages. Elevation of the basin ranges from 102 m to 659 m ASL. The entire area of the basin is characterised by undulating terrain and scattered residual hills of granitic rock mounds (Das *et al*., 2020). Unconsolidated sediments of the recent age are deposited through the area of the river channel whereas most of the basin area is underlain by the Precambrian metamorphic rocks. The temperature ranges from 6°C (January) to 43°C (May) and the south-west monsoon brings rain to the basin predominantly from June to September with an average rainfall of 110-150 cm whereas the highest temperature is attained during May (43°C) and the lowest temperature

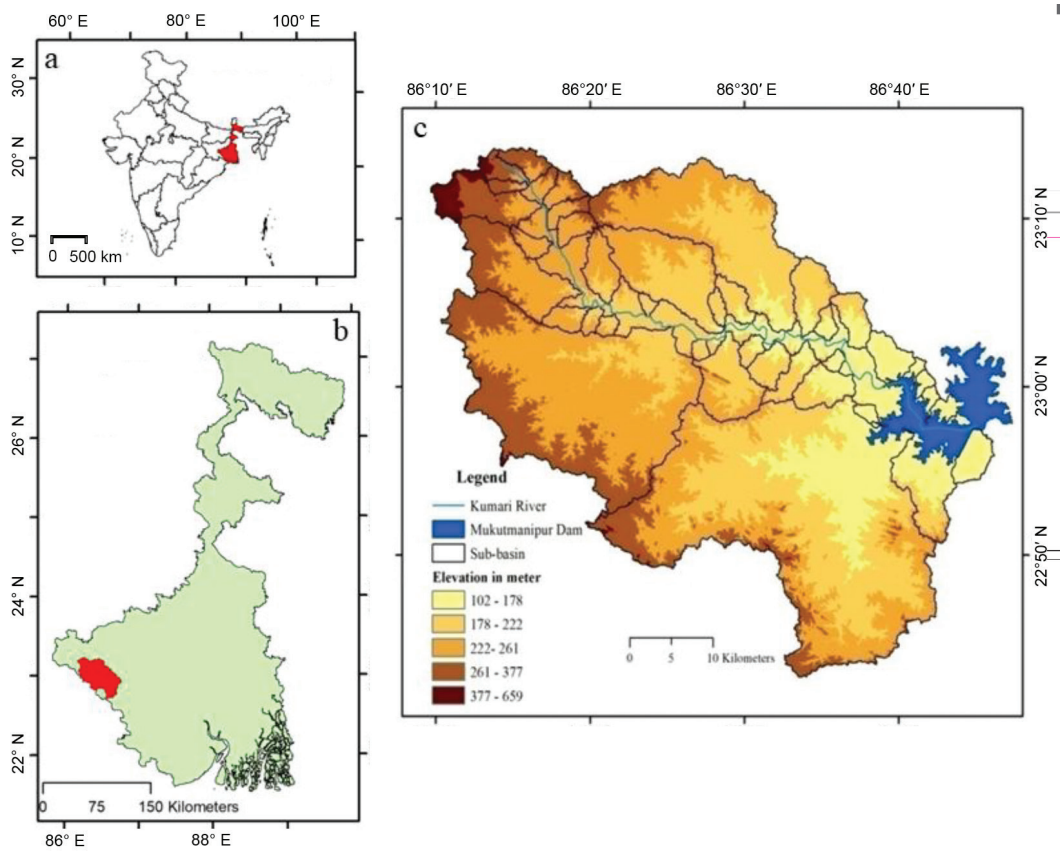

Figure 1. Location of the studied basin a) Location of India and the state of West Bengal in India b) Location of Kumari basin within West Bengal c) DEM of the Kumari basin showing the main channel.

in January (6°C). On the other hand, light textured and shallow to moderately deep and intense erosion-susceptible soil dominates the entire catchment except the Ajodhya and Dalma Hilly Region.

Methodology

The Revised Universal Soil Loss Equation is an empirical model that takes into consideration the terrain, climate, presence or absence of vegetation and anthropogenic interference. The RUSLE model is basically a modified version of the Universal Soil Loss Equation (USLE), originally suggested by Wischmeier and Smith (1978) in the United States Department of Agriculture (USDA) Handbook Number 537.

The RUSLE Model

The RUSLE model efforts to estimate the annual loss of topsoil from an areal unit based on specific conditioning factors, including both physical and anthropogenic. This can be expressed as follows (Renard *et al*., 1997)

$$A = R \times K \times LS \times C \times P \qquad \text{Equation 1}$$

where, A is the average annual soil loss in an areal unit (ton ha^{-1} yr^{-1}), R is the average annual rainfall erosivity factor (MJ mm ha^{-1} h^{-1} yr^{-1}), K is the soil erodibility factor (t h MJ^{-1} mm^{-1}), LS corresponds to the dimensionless factor associated with slope-length and slope-steepness, respectively, C is the vegetation cover factor and P is the conservation support practice factor.

Rainfall Erosivity Factor (R)

Most of the water-induced erosion experienced in an areal unit is tremendously sensitive to runoff. It is a well-known fact that the runoff depends on the rainfall occurring in an areal unit and hence the rainfall-runoff erosivity turns out to be an important parameter in the RUSLE Model. In addition to the amount of rainfall, different secondary factors such as the intensity of rainfall, terminal velocity, and raindrop size and distribution have a significant effect on the total erosivity of rainfall (Blanco-Canqui and Lal, 2008). In a particular area, the average storm surges often regulate the soil erosion potentiality (Das *et al*., 2018). The determination of the R factor depends on the product of the total rainfall energy (E) and the maximum 30 min rainfall intensity (I30) and its long-term average. The amount of rainfall-induced runoff quantifies the numerical value of R (Wischmeier and Smith, 1978; Renard *et al*., 1997). Here it is informed that the 30 min rainfall intensity data is not available in most parts of the world. Therefore, in these circumstances, the traditional definition of R factor cannot be used. Tyndall Climatic Data provides the monthly rainfall from the years 1901 to 2018 (Mitchell *et al*., 2002). So, this highly accurate climatic data for the years 2014 to 2018 have been employed for the extraction of R factor. For the calculation of the R factor in this article, amongst a variety of proposed equations from literature (Renard and Freimund, 1994; Lee and Heo, 2011), the Modified Fournier Index (MFI) stated by Arnoldus (1997) has been used which is represented in Eq. 2 and Eq. 3.

$$R = 1.735 \times \log_{10}[1.5\log_{10}(MFI) - 0.8188] \qquad \text{Equation 2}$$

$$MFI = \frac{\sum_{i=1}^{12} p_i^2}{Pa} \qquad \text{Equation 3}$$

where, MFI = Modified Fournier Index, pi is the monthly rainfall (in mm) and Pa is the annual rainfall (in mm).

Soil Erodibility Factor (K)

It is a well-known fact that rainfall-induced runoff cannot spontaneously

affect soil erosion because the nature and intensity of runoff are highly controlled by the behavior of the underlying soil or rock of the watershed, whereas runoff can be reduced due to the existence of underlying high infiltration capacity soil or rocks, consequently, the amount of erosion/ topsoil removal gets reduced. Therefore, it can be stated that the soil erodibility factor (K factor) is highly sensitive to the different physical and chemical pedologic properties such as texture, organic matter, soil reaction, etc. (Wischmeier and Smith, 1978; Atoma *et al*., 2020). This K Factor refers to the capacity or the power to transport soil particles by the energy of rainfall-induced runoff (Haile and Fetene, 2012). However, the power/capacity of transportation is highly dependent on the inherent characteristics of the soil which may be called soil erodibility.

In this paper, a combination of field and laboratory-based analysis has been employed to extract the K factor. The entire Kumari basin was divided into 2 km × 2 km grids (Fig. 2) to collect the soil samples from the gridline intersecting points. These collected soil samples have been tested in the laboratory to obtain texture, organic matter status, and pH by performing the sieve and Walkley-Black methods, respectively. Soil reaction was also measured with a pH Meter. All these were employed in Equation 3 in order to derive the K factor (David, 1988).

$$K = (0.043 \times pH) + (0.62 \div OM) + (0.0082 \times S) - (0.0062 \times C) \times Si$$

Equation 4

where, K is soil erodibility (t h $MJ^{-1}mm^{-1}$), pH is the acidity/alkalinity of the soil, OM is Organic matter (%), S is Sand content (%), Si is silt content (%), C is clay ratio i.e. % Clay/ (% Sand + % silt)

Slope Length and Steepness Factor (LS)

Slope length (L) and slope steepness (S) are the most significant topographic attributes determining the soil susceptibility to erosion, and become important components as defined as the product of the factors of slope length (L) and slope steepness (S) in the RUSLE Model

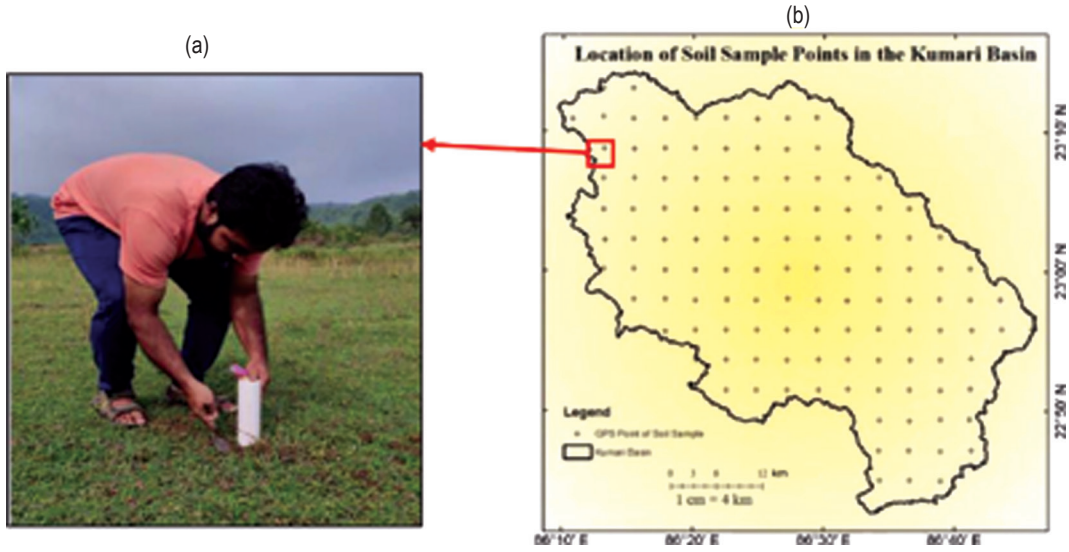

Figure 2. a) Soil sample collection at Mudali village. b) Grid sampling points (with the location of the Mudali Village shown by a red square and arrow) for soil sample collection in the Kumari river basin..

of annual soil loss (Prasannakumar *et al*., 2012). Normally, areas with steep slopes are more erosion-prone than flat or gently sloped areas. Similarly, longer slopes facilitate soil erosion, therefore, soil erosion increases with increasing slope lengths and vice versa. This indicates the sensitivity of topographic parameters to soil loss; therefore, appropriate derivation of this feature is considered a requirement. In general, the slope steepness (S Factor) is more pertinent as compared to the slope length (L Factor) (Wischmeier and Smith, 1978). Slope length (L) can be defined as the horizontal distance from the base of the overland flow to the specified point and the slope (S) is defined as the slope angle. Renard *et al*. (1997) defined the LS factor as the ratio between a given slope length and slope steepness (LS) to foretell the soil loss of an area under consideration. Although the LS Factor is generally calculated at the level of the agricultural field, this method is not suitable for basin and catchment scale. With the discovery of Digital Elevation Models (DEMs), this problem is minimised using the Flow Accumulation Routine in a GIS environment (Van Remortel *et al*., 2001; Zhang *et al*., 2013). The LS Factor also depends on the flow accumulation, the flow direction and terrain character of the catchment area (Wischmeier and Smith, 1978). The LS factor, based on the equations developed by Wischmeier and Smith (1978) and Moore and Burch (1986), has been widely used by Griffin *et al*., (1988), McCool *et al*. (1989) and Moore and Wilson (1992). According to Hrabalíková and Janecek (2017), the DEM-based LS factor, computed in a GIS environment, is usually 10-30% lesser than the values obtained by the manual method.

This study has used the equation proposed by Moore and Burch (1986) using the 30m resolution SRTM DEM in ArcGIS environment (Eq. 5).

$$LS = \left(\frac{As}{22.13}\right)^{0.6} \times 1.4 \left(\frac{\sin^1 B}{0.0894}\right)^{1.3} \quad \text{Equation 5}$$

where, LS = LS Factor, As = Flow Accumulation Raster and B = Slope in radians.

Crop Management Factor (C)

C-factor is an important erosion factor that can be easily affected by anthropogenic activities to reduce erosion (McCool *et al*., 1995). It is defined as the ratio of soil loss under certain cropping conditions to soil loss that occurs in bare soil (Wischmeier and Smith, 1978). The C-factor reflects the outcome of vegetal cover and its amount and type on the rate of annual soil loss (Uddin *et al*., 2016).

With the availability of the high-resolution remotely sensed database, different remote sensing-based techniques like LULC classification (Millward and Mersey, 1999), spectral indices (Meusburger *et al*., 2010; Puente *et al*., 2011; Vijith *et al*., 2017) etc. are now preferred over the traditional techniques as low cost, rapid and relatively appropriate data analysis (Durigon *et al*., 2014) to compute the C factor.

The use of spectral indices has been increased by many researchers to evaluate the fraction of vegetation and its influence on the C-factor values (Puente *et al*., 2011). These include the Normalised Difference Vegetation Index (NDVI) and other indices. The primary advantage of using spectral indices is that these indices, which are solely based on band ratios, negate the effect of atmosphere, moisture, and LULC (Meusburger *et al*., 2010).

Several empirical equations have been manifested by different researchers to relate vegetation index values to the C-factor value.

These equations have widely been employed in many watersheds across the world (Uddin *et al*., 2016) to assess soil erosion. The empirical equation formulated by Van der Knijff *et al*. (2000) has been employed by a host of researchers to derive the RUSLE C-factor from NDVI in different watersheds.

In this research, to derive the RUSLE-based C-factor from NDVI, this empirical equation has been employed as follows:

$$C\ factor = Exp\ [-\acute{\alpha} \times NDVI / (\beta - NDVI)] \quad \text{Equation 6}$$

where ά and β parameters determine the shape of the NDVI curve.

The equation for the calculation of NDVI is as follows:

$$NDVI = (NIR-R) / (NIR+ R) \quad \text{Equation 7}$$

where NIR = Near Infrared band and R = Red band.

For the calculation of the C Factor, the USGS-derived Landsat 8 images (OLI) downloaded for the year 2019 were used. In the OLI images, Band 4 is the Red band, Band 5 is the NIR band, and Band 6 is the SWIR band.

Support Practices Factor (P)

In general, the P-factor and C-factor are both related as they are designed to specify the positive impact of management practices in decreasing soil erosion (Toy *et al*., 1999; Renard *et al*., 2011). However, the P-factor is distinguishable from the C-factor as it recommended the control of runoff through the impact of management, by and large how the adopted management practices such as contour tillage, strip cropping, and terraces reduce and modify the pattern and speed of runoff (Renard and Foster, 1983; Renard *et al*., 1997, 2011).

In this exercise, the LULC map was used, which was processed by the supervised classification in the ArcGIS environment. According to the USDA Handbook No.282 (1981) (Table 1) the values of the P factor were assigned to different LULC classes (Wischmeier and Smith, 1978; Renard *et al*, 1997). The P Value ranges from 0 to 1 and is based on the land use categories.

After the evaluation of all the quantitative parameters of RUSLE and confirmation that all the rasters were of the same spatial resolution, the annual soil loss was computed in the Arc GIS platform (Arc GIS 10.2.2). The product of all parameters of RUSLE has been calculated by using the Raster Calculator Module of the Spatial Analyst Tools in Arc GIS to estimate the pixel-by-pixel annual soil loss (ton ha^{-1} yr^{-1}) in the Kumari basin.

Table 1. Values of P factor respected Land use/ Land cover type. (Source: USDA Handbook No 282).

Type	Value
Dense Vegetation	0.8
Light Vegetation	0.8
Built-up Area	2.0
Agricultural Land	0.5
Waterbody	1.0
Fallow Land	0.9

For ascertaining the spatial variation in the R factor of the Kumari watershed, equation 2 and 3 were employed. It is evident that the equation requires the data for monthly rainfall as well as annual rainfall. It has been stated earlier that, in this exercise, the rainfall data were obtained from the Tyndall Climatic Archive (Mitchell *et al*., 2002). The ratio between the average monthly and the annual rainfall gives the month-wise MFI which were then cumulated for all the months to get the annual MFI for the studied basin (Fig. 3a). This MFI was used in Eq. 2 to get the spatial variation in the R factor (Fig. 3b) across the study area.

Results and discussion

Rainfall Erosivity Factor (R)

For ascertaining the spatial variation in the R factor of the Kumari watershed, equation 2 and 3 were employed. It is evident that the equation requires the data for monthly rainfall as well as annual rainfall. It has been stated earlier that, in this exercise, the rainfall data were obtained from the Tyndall Climatic Archive (Mitchell *et al*., 2002). The ratio between the average monthly and the annual rainfall gives the month-wise MFI which were then cumulated for all the months to get the annual MFI for the studied basin (Fig. 3a). This MFI was used in Eq. 2 to get the spatial variation in the R factor (Fig. 3b) across the study area.

Soil Erodibility Factor (K)

Usually, the pedologic characteristics (i.e., soil organic matter, soil pH, and soil texture) of the watershed actively influence the soil erodibility factor ('K'-factor) (Fig. 4 a – e). The spatial variation of K-factor scores of the Kumari watershed has been obtained by employing the Equation 4. According to the K Factor map of the Kumari basin, it is evident that the average value of the K Factor is about 0.182 whereas it ranges from 0.160 to 0.207. It is evident that the K Factor increases in a NW-SE trend, fact that, it is more or less similar to the clay map. The map displays comparatively higher values of the K Factor which is highly concentrated in the southeastern and eastern domains of the Kumari basin which is the area along the entire Jamuna (a tributary of Totko-Jam) river basin. In this domain, the clay content is high along with lower organic matter which prevents the formation of clay-humus-complex. Under these circumstances, the permeability of the soil does not increase much which leads to high runoff character (Roy and Sengupta, 2019). So, the particle detachment on the lower domain can easily take place due to splash erosion and surface runoff. By and large, soils are more vulnerable to erosion in this region. On the other hand, the upper domain (N-W portion) especially the area of foothills and its surrounding areas

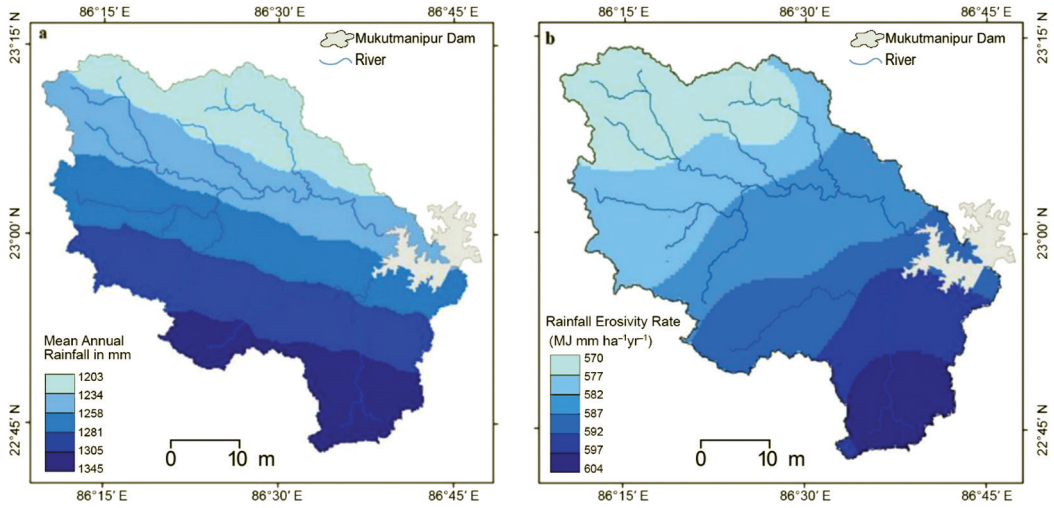

Figure 3. The Kumari basin: Spatial variation of a) Mean annual rainfall, b) Rainfall erosivity rate..

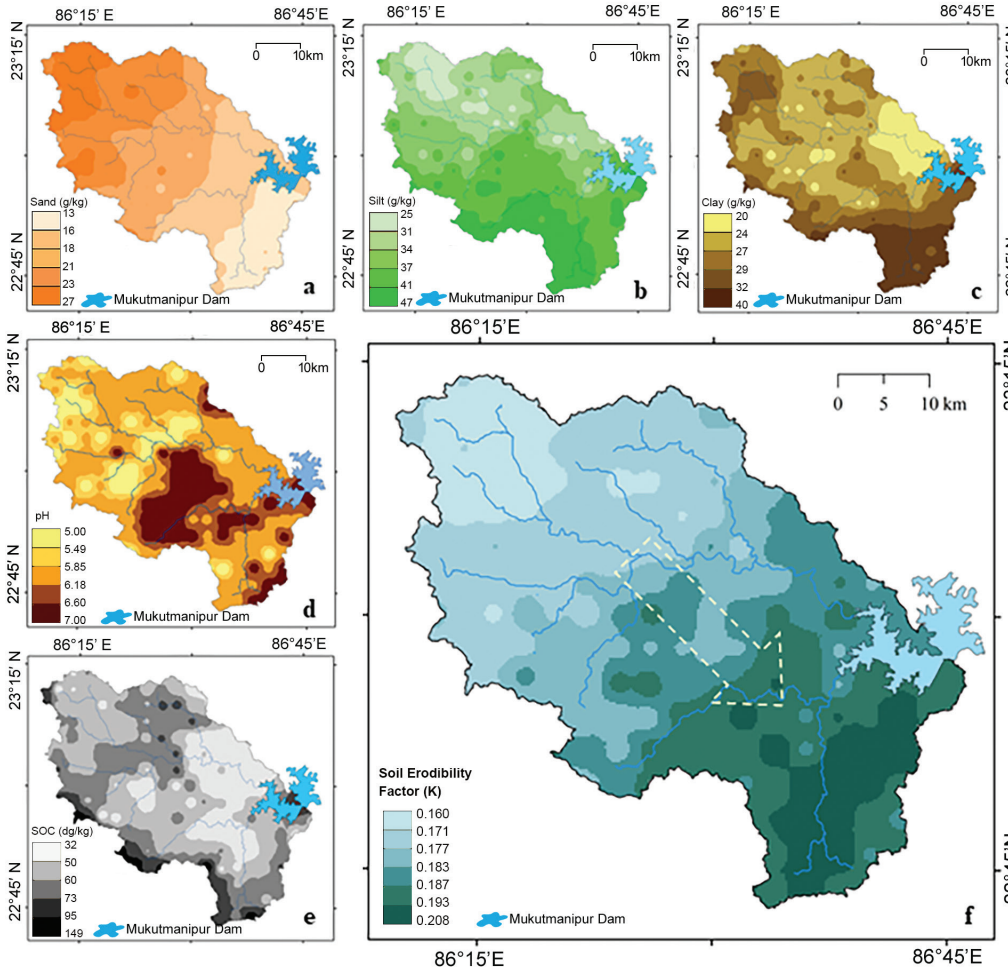

Figure 4. (a-e). Pedological attributes of the Kumari basin. a) Sand, b) Silt, c) Clay, d) Soil organic matter, e) pH map; f) K-factor variation..

is characterised by low values of K Factor because the sand content is high.

Slope length and steepness factor (LS)

The LS Factor has a direct impact on soil loss estimation. This is because it is derived from factors that affect the course and direction of surface runoff. In other words, the direction and flow/movement of the major agents of erosion is highly controlled by the LS Factor. The spatial variation of the LS Factor of the Kumari basin has been extracted from the flow accumulation raster (Fig. 5b) and the slope in degrees (Fig. 5a) by applying Equation 5. In this study area, the average value of the LS factor is 0.109 whereas it ranges from 0.00 to 20.09. The entire basin has been characterised by very low values of LS Factor except for some scattered and isolated high values (>10) of LS Factor distributed corresponding to the high slope areas along the Ajodhya, Dalma

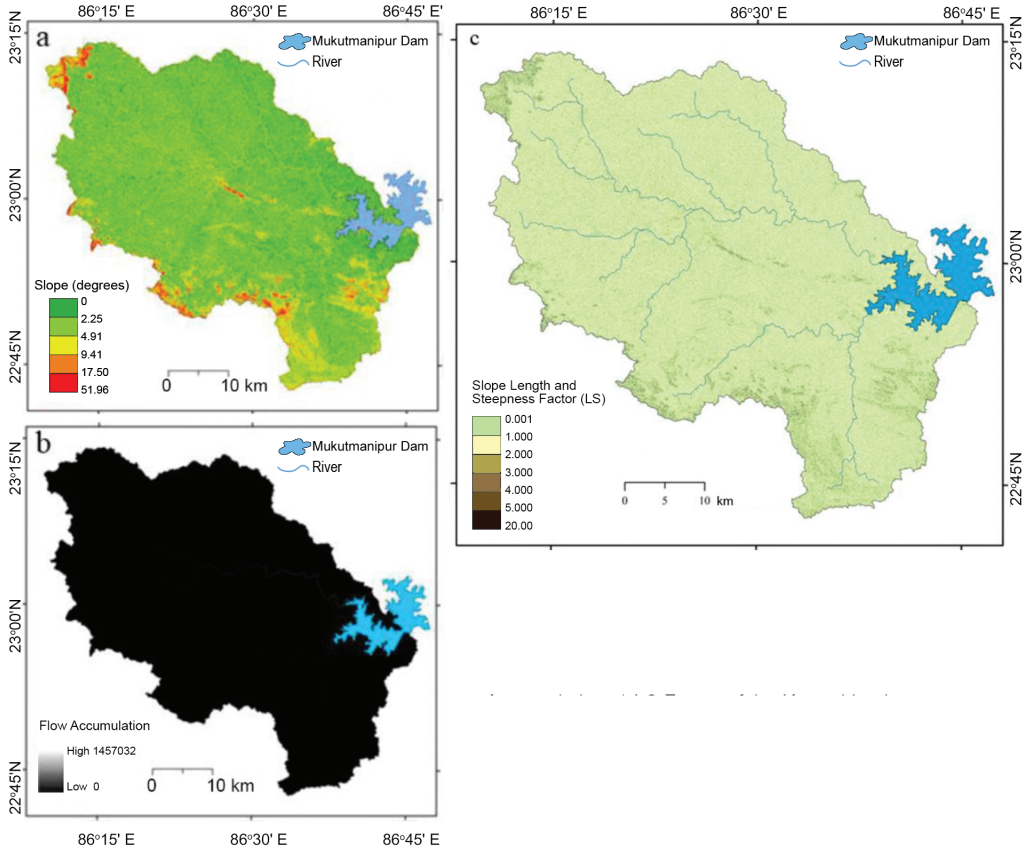

Figure 5. Spatial variation rasters of a) slope b) flow accumulation c) LS factor of the Kumari basin..

hilly tract, and a residual hilly region of the middle domain of the Kumari basin (Fig. 5c).

Crop Management factor (C)

It is a known fact that the existence of vegetation restricts soil erosion by decreasing the amount of surface runoff and splash erosion. Therefore, it is imperative that the vegetal canopy needs to be taken into consideration apart from the physical factors such as rainfall, slope, and soil. In this paper, the RUSLE-derived C Factor is calculated from the NDVI (Fig. 6a) by employing the empirical Eq. 6.

From the Map (Fig. 6b) displaying the C factors of the Kumari watershed, it is evident that the C-factor score ranges from 0 to 1.01 with an average value of 0.396. The high C-factor is concentrated in the area of the less vegetated and barren lands whereas the low C Factor is observed in the areas of dense vegetation.

Support Practice factor (P)

The range of the P-factor varies from 0 to 1. It is well recognised that areas of better land management are associated with a lower magnitude of the P factor, and therefore a lower degree of erosion and vice versa. The landuse landcover (LULC) map was extracted from the Landsat OLI data by employing the Supervised Classification in ArcGIS.

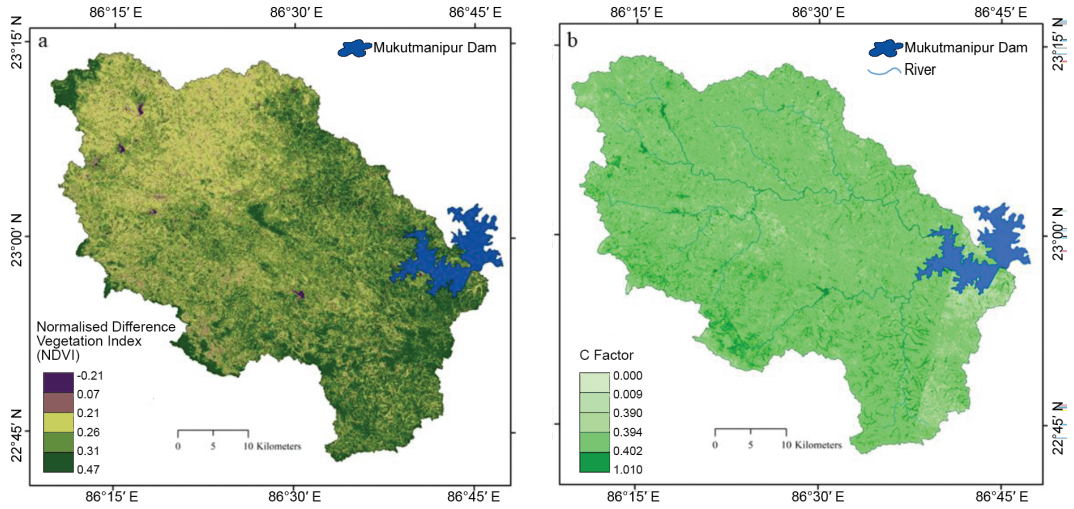

Figure 6. Kumari basin: Variation in the NDVI (a) and C Factor (b).

The entire LULC for the Kumari basin was divided into five major categories viz., water body, barren land, built-up area, vegetation, and agricultural land (Fig. 7a) to estimate the P-factor. The values of the P Factor were assigned in accordance with Table 1 for each corresponding LULC category. In the next part, the Look Up command in Arc GIS was run to the LULC raster in order to assign the values of the P Factor concerning the LULC category as per Table 1 given by USDA.

It was also made sure that all the rasters were of the same resolution. So, the P Factor map as well as the conditioning rasters of RUSLE was resampled to the same resolution i.e., 30 m. Fig. 7b displays the spatial variation in the magnitude of the P-factor, wherein the mean P Factor is 0.852, and the range of this factor varies from 0.50 to 1.0. A glimpse of the map reveals that a large proportion (66.04 %) of the land in the basin area is covered by agricultural field and the upper domain is covered by barren land. The high values are found in the North West section of the basin, whereas low values of P are concentrated in the South East section. By and large, low values of P are associated with the highlands and densely vegetated areas.

Estimating the annual soil loss

In the Kumari drainage basin, annual soil losses are estimated by employing the Revised Universal Soil Loss Equation (RUSLE). This empirical model incorporates several factors (viz., R, K, LS, C, and P) that determine the rate of annual soil erosion. The spatial variation of the aforesaid factors has already been discussed and demonstrated earlier. The rasters of all such causal factors have gone through the multiplication process in the Raster Calculator Module of Arc GIS in order to obtain the raster of estimated soil loss by the RUSLE method.

Annual soil loss of the Kumari basin

The estimated annual soil loss ranges from <5 to <80 ton ha^{-1} yr^{-1} with a mean soil loss of 1.766 ton ha^{-1} yr^{-1}. Based on the Natural Breaks Method, the annual soil erosion map of the studied basin has been divided into six classes: very low (< 5 ton ha^{-1} yr^{-1}), low (5 – 10 ton ha^{-1} yr^{-1}), moderate (10 – 20 ton

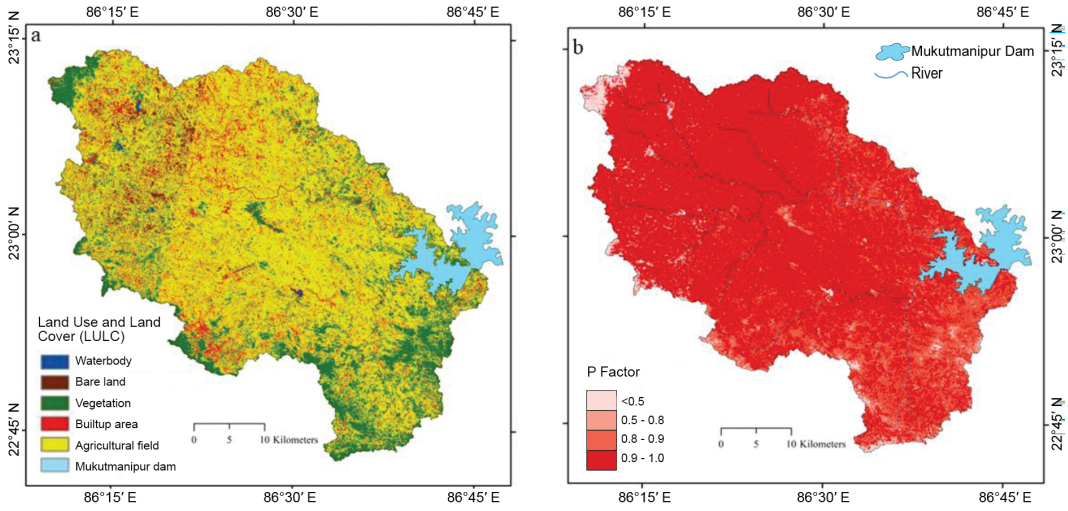

Figure 7. Spatial variation in The Kumari basin: a = LULC, b = support practice factor (P).

ha^{-1} yr^{-1}), high (20 – 40 ton ha^{-1} yr^{-1}), very high (40 – 80 ton ha^{-1} yr^{-1}), extremely very high (>80 ton ha^{-1} yr^{-1}). On the other hand, it is evident that about 16.36% of the area in the Kumari river basin experiences annual soil losses greater than 10 ton ha^{-1}yr^{-1}. According to the FAO (2017) guideline, this is reasonably high, and sustainable land management is essentially needed in this region. Such areas of high estimated soil loss are predominantly concentrated in the highland region especially the hills of Ajodhya and Dalma (Fig. 8a).

Table 2. Kumari basin: Soil erosion classes and the percentage of villages in each class.

Soil loss (ton ha^{-1} yr^{-1})	Erosion classes	Villages in %
<5	Very Low	47.58
5-10	Low	36.06
10-20	Moderate	10.49
20-40	High	4.37
0-80	Very High	1.48
>80	Extremely High	0.02

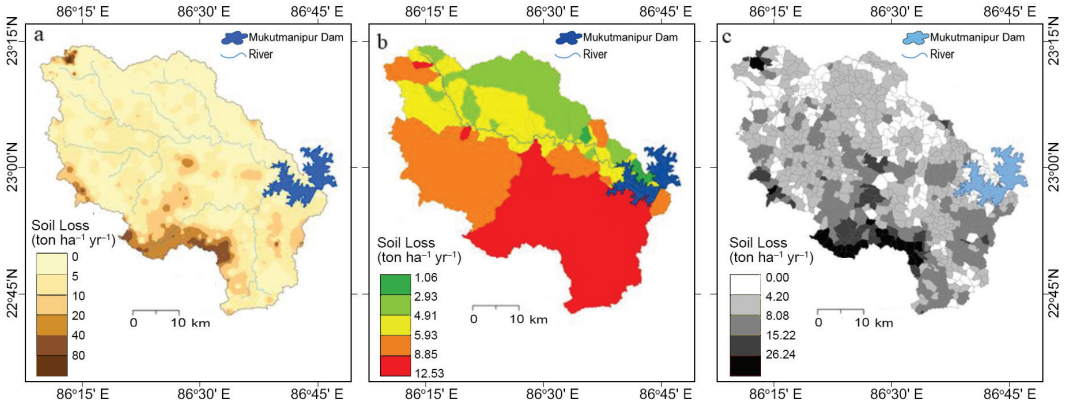

Figure 8. Spatial variation in the Kumari basin a) Annual soil loss, b) Sub-basin wise soil loss c) Village wise soil loss..

Another important observation that can be specified in Fig. 8a is that the annual soil loss in the Kumari river basin is low to very low. (<10 ton ha^{-1} yr^{-1}) except in the area of the hilly tracts of Ajodhya (upper domain of the Kumari river) and Dalma (upper domain of the Totko-Jam basin) with the isolated hill near the village of Fulijhor in the middle domain.

Sub-basin wise annual soil loss of the Kumari basin

So, from the above analysis, it is clear that there are many parts in the Kumari basin where the estimated soil loss is significantly higher and hence proper management strategies are needed in the region. However, in a resource scarce scenario, it is important to prioritize certain areas where management strategies need to be employed urgently. For this purpose, sub-basin wise soil loss may be helpful in assigning priority ranks. So, the next part of this study included the estimation of soil loss in the sub-basins of the Kumari basin. The raster of annual soil loss of the Kumari basin was processed through the Zonal Statistics as table routine (statistics type- mean) in the Spatial Analyst Tools of Arc GIS in order to carry out the sub-basin level annual soil loss vector, illustrating the sub-basin level spatial variation of mean annual soil loss in the Kumari river basin (Fig. 8b). Among the 36 sub-basins, the number in each category of erosion susceptibility (very low, low, moderate, high and very high) is 4, 10, 8, 9 and 5, respectively. One of the apparent confusions that is evident is that although the Kumari basin is categorised into 36 sub-basins, the relative area under each sub-basin is not uniform. For example, the areal extent of the Totko-Jam basin is much greater as compared to the counterparts in the upper section. The physiography of the studied basin is such that the right bank tributaries are much more extensive compared to their counterparts in the left bank. This scenario of mismatching areas is due to the fact that we have taken only those sub-basins as an areal unit provided it directly meets with the Kumari and the order of the trunk stream is at least 3. Therefore, the areas encompassed under each sub-basin is not uniform.

Even a casual look at Fig. 8b reveals that the sub-basins DMDR041R017, DMDR041R010, DMDR041R006, DMDR041R001, and DMDR041R018 are characterised by high annual soil loss. The possible reason for this (R-L) distribution is that the right bank (RB) sub-basins have greater area, higher R-factor, and higher clay content (K-factor) as compared to the left bank (LB) sub-basins. The naming of the sub-basins is in coherence with the methodology proposed by the River Basin Atlas of India (Dadhwal *et al*., 2012). Since the Kumari is a tributary of the Kangsabati, which, in turn meets the Damodar. Hence, the Kumari basin is a part of the broader Damodar basin and hence named accordingly.

Village-wise annual soil loss of the Kumari basin

It has been stated in the previous section that the relative areal extent of the sub-basins is not uniform. In order to counteract this possible bias in prioritisation due to differing basin sizes, the village-level prioritisation has been attempted. It is expected that the villages (942 in number) are of, more or less, equal extent. Furthermore, in a country like India, administrative boundaries are rarely constructed concerning the natural/ physical boundary. Rather, in India, villages represent the smallest administrative unit. So, it is expected that all the management decisions will be implemented by the village

administration. So, it is expected that if such a comprehensive database of the average soil loss in all the 942 villages of the studied basin is available, the decision-making process would be extremely simple. The same procedure that was applied for extracting the sub-basin level soil loss was used to detect the village-level annual soil loss. According to Fig. 8c, the village-level estimated mean annual soil loss ranges from 0.00 to 40.41 ton ha^{-1} yr^{-1} with the average being 7.71 ton ha^{-1} yr^{-1}. The number of villages falling under each category of soil loss have been displayed in Table 2. It is apparent that, high-erosion villages are found in and around hilly tracts of Ajodhya and Dalma.

Conclusion

Systematic soil loss data needs to be available to the government agencies so that sustainable conservation practices can be planned. This becomes very important in a country like India wherein the resource availability is limited to some extent and therefore, prioritization appears to be an effective solution in resource scarce scenarios. Among the various sub-basins, the Totko-Jam Sub-basin in the right bank (represented by red shades in Fig. 8b) shows higher erosion susceptibility. The high erosion potentiality in this basin is possibly due to higher values of erodibility (K Factor) consequent to high clay and low organic matter content. This prevents the formation of a rich clay-humus complex. Among the villages, most of the villages on the right bank sub-basins display a greater amount of soil loss. This is especially true for the villages in the areas of the hilly tracts of Ajodhya and Dalma which represent very high annual soil loss. Therefore, it is expected that conservation techniques need to be highly prioritised in this region. And this calls for immediate action as apart from the agricultural perspective, the problem of dam siltation also assumes greater significance considering the fact that the Mukutmanipur Dam is located in the vicinity.

References

Arnoldus, H.M.J. (1997) Methodology used to determine the maximum potential average annual soil loss due to sheet and rill erosion in Morocco. *Food and Agricultural Organization Soils Bulletin,* 5: 39–48.

Atoma, H., Surtabhagavan, K.V. and Balakrishan, M. (2020) Soil erosion assessment using RUSLE model and GIS in Huluka watershed, Central Ethiopia. *Sustainable Water Resource Management,* 6(1): 1–17. http://dx.doi.org/10.1007/s40899-020-00365-z.

Blanco-Canqui, H. and Lal, R. (2008) *Principles of soil conservation and management,* 1st Ed, Springer, Netherlands: 617p.

Borrelli, P., Robinson, D.A., Fleischer, L.R., Lugato, E., Ballabio, C., Alewell, C., Meusberger, K., Modugno, S., Schutt, B., Ferro, V., Bagarello, V., Van Oost, K., Montanarella, L. and Panagos, P. (2017) An Assessment of the Global Impact of 21st Century Landuse Change on Soil Erosion. *Nature Communication,* 8, 2013: 1–13. http://doi.org/10.1038/s41467-017-02142-7.

Buendia, C., Bussi, G., Tuset, J., Vericat, D., Sabater, S., Palau, A. and Batalla, R.J. (2016) Effects of afforestation on runoff and sediment load in an upland Mediterranean catchment. *The Science of the Total Environment,* 540: 144–157.

Butt, M.J., Waqas, A. and Mahmood, R., CSHRG (2010) The combined effect of vegetation and soil erosion in the water resource management. *Water Resources Management,* 24(13): 3701–3714. http://dx.doi.org/10.1007/s11269-010-9627-7.

Chou, W.C. (2010) Modelling watershed scale soil loss prediction and sediment yield estimation.

Water Resources Management, 24(10): 2075–2090.

Dadhwal, V.K., Kumar, R., Sharma, J.R., Tembhurney, W.M., Bera, A.K., Paithankar, Y., Paliwal, R., Kalsi, A.P., Chauhan, N., Bhati, G., Shirsath, Paresh B., Bankar, N., Sharma, V. and Singh, H. (2012). *River Basin Atlas of India,* Government of India Ministry of Water Resources: 144p.

Das, B., Paul, A., Bordoloi, R., Tripathi, O.P. and Pandey, P.K. (2018) Soil erosion risk assessment of hilly terrain through integrated approach of RUSLE and geospatial technology: a case study of Tirap District, Arunachal Pradesh. *Modelling Earth Systems and Environment,* 4(1): 373–381.

Das, S., Roy, S. and Sengupta, S. (2020) Drainage basin morphometry and its relation to erosion susceptibility in the Barakar river basin, Jharkhand and West Bengal. *Journal of Indian Geomorphology,* 8: 73–89.

David, W.P. (1988) *Soil and water conservation planning: Policy Issues and Recommendations. Journal of Philippine Development,* 26(XV): 47–84.

Durigon, V.L., Carvalho, D.F., Antunes, M.A.H., Oliveira, P.T.S. and Fernandes, M.M. (2014) NDVI time series for monitoring RUSLE cover management factor in a tropical watershed. *International Journal of Remote Sensing,* 35: 441–453. http://doi.org/10.1080/01431161.2013.871081.

Dutta, M., Saikia, J., Taffarel, S.R., Waanders, F.B., de Medeiros, D., Cutruneo, C.M.N.L., Silva, L.F.O. and Saikia, B.K. (2017) Environmental assessment and nano-mineralogical characterization of coal, overburden, and sediment from Indian coal mining acid drainage. *Geoscience Frontiers,* 8(6): 1285–1297. http://doi.org/10.1111/j.1600-0587.2012.07348.x.

Farhan, Y., Zregat, D. and Farhan, I. (2013) Spatial estimation of soil erosion risk using RUSLE approach, RS, and GIS techniques: a case study of Kufranja Watershed, Northern Jordan. *Journal of Water Resource and Protection,* 5(12): 1247–1261. https://doi.org/10.4236/jwarp.2013.512134.

Gebremicael, T.G., Mohamed, Y.A., Betrie, G.D., Zaag, P. and Teferi, E. (2013) Trend analysis of runoff and sediment fluxes in the Upper Blue Nile basin: a combined analysis of statistical tests, physically based models and land-use maps. *Journal of Hydrology,* 482: 57–68. https://doi.org/10.1016/j.jhydrol.2012.12.023.

Griffin, M.L., Beasley, D.B., Fletcher, J.J. and Foster, G.R. (1988) Estimating soil loss on the topographically non-uniform field and farm units. *Soil Water Conservation,* 43: 326–331.

Haile, G.W. and Fetene, M. (2012) Assessment of soil erosion hazard in Kilie catchment, East Shoa, Ethiopia. *Land Degradation and Development,* 23(3): 293–306.

Hoyos, N. (2005) Spatial modeling of soil erosion potential in a tropical watershed of the Colombian Andes. *Catena,* 63: 85–108. https://doi.org/10.1002/ldr.1082.

Hrabalíková, M. and Janeček, M. (2017) Comparison of different approaches to LS factor calculations based on a measured soil loss under simulated rainfall. *Soil and Water Research,* 12: 69–77.

Jasrotia, A.S. and Singh, R. (2006) Modeling runoff and soil erosion in a catchment area, using GIS, in the Himalayan region, India. *Environmental Geology,* 51: 29–37.

Kim, J., Choi, J., Choi, C. and Park, S. (2013) Impacts of changes in climate and land use/land cover under IPCC RCP scenarios on streamflow in the Hoeya River Basin, Korea. *The Science of the Total Environment,* 452-453: 181–195. http://doi.org/10.1016/ j.scitotenv.2013.02.005.

Kim, J.B., Saunders, P. and Finn, J.T. (2005) Rapid assessment of soil erosion in the Rio Lempa Basin, Central America, using the Universal Soil Loss Equation and Geographic Information Systems. *Environmental Management,* 36: 872–885. http://doi.org/10.1007/s00267-002-0065-z.

Lee, J-H. and Heo, J-H. (2011) Evaluation of estimation methods for rainfall erosivity based on annual precipitation in Korea. *Journal of Hydrology,* 409(1-2): 30–48. http://dx.doi.org/10.1016/j.jhydrol.2011.07.031.

Lee, S. (2004) Soil erosion assessment and its verification using the Universal Soil Loss Equation and Geographic Information System: A case study at Boun, Korea, *Environmental Geology,* 45: 457–465.

Lim, K.J., Sagong, M., Engel, B.A., Tang, Z., Choi, J. and Kim, K.S. (2005) GIS-based sediment assessment tool. *Catena,* 64(1): 61–80. http://doi.org/10.1016/ j.catena.2005.06.013.

Lin, C.Y., Lin, W.T. and Chou, W.C. (2002) Soil erosion prediction and sediment yield estimation: the Taiwan experience. *Soil and Tillage Research,* 68(2): 143–152.

Lorup, J.K. and Styczen, M. (1996) Soil Erosion Modeling. In Abbott, M.B. and Refsgaard, J.C. (eds.) *Distributed Hydrological Modelling,* Kluwier Academic Publishers: 93–120.

McCool, D.K., Foster, G.R., Mutchler, C.K. and Meyer, L.D. (1989) Revised slope length factor for the Universal Soil Loss Equation. *Transactions of the ASAE*, 32: 1571–1576.

McCool, D.K., Foster, G.R., Renard, K.G. and Weesies, G.A. (1995) The revised universal soil loss equation. *Proceedings of DOD Interagency Workshop on Technologies to Address Soil Erosion on DOD Lands,* San Antonio, Department of Defence. https://www.tucson.ars.ag.gov/unit/publications/PDFfiles/1132.pdf (retrieved on 2024-02-01).

Meusburger, K., Bänninger, D. and Alewell, C. (2010) Estimating vegetation parameter for soil erosion assessment in an alpine catchment by means of QuickBird imagery. *International Journal of Applied Earth Observation and Geoinformation,* 12: 201–207. http://doi.org/10.1016/j.jag.2010.02.009.

Millward, A.A. and Mersey, J.E. (1999) Adapting the RUSLE to model soil erosion potential in a mountainous tropical watershed. *Catena,* 38: 109–129. http://doi.org/10.1016/S0341-8162(99)00067-3.

Mitchell, T.D., Hulme, M. and New, M. (2002) Climate data for political areas. *Area,* 34:109–112.

Moore, I.D. and Burch, G.J. (1986) The physical basis of the slope factor in the universal soil loss equation. *Soil Science Society of America Journal,* 50: 1294–1298.

Moore, I.D. and Wilson, J.P. (1992) Length-slope factors for the revised universal soil loss equation: simplified method of estimation. *Journal of Soil and Water Conservation,* 47(5): 423–428.

Mutua, B.M., Klik, A. and Loiskandl, W. (2006) Modelling soil erosion and sediment yield at a catchment scale: the case of Masinga Catchment, Kenya. *Land Degradation and Development,* 17: 557–570.

Oliveira, P.T.S., Almagro, A., Thomé, T.C., Colman, C.B., Pereira, R.B., Junior, J.M. and Rodrigues, D.B.B. (2019) *Soil Erosion and Sediment Yield Estimating on Multiple Spatial and Temporal Scales.* In AGU Fall Meeting 2019. AGU.

Pandey, A., Mathur, A., Mishra, S.K. and Mal, B.C. (2009) Soil erosion modelling of a Himalayan Watershed using RS and GIS. *Environmental Earth Sciences,* 59: 399–410.

Prasannakumar, V., Vijith, H., Abinod, S. and Geetha, N. (2012) Estimation of soil erosion risk within mountainous sub-watershed in Kerala, India, using Revised Universal Soil Loss Equation (RUSLE) and geo-information technology. *Geoscience Frontiers,* 3(2): 209–215. http://doi.org/10.1016/j.gsf.2011.11.003.

Puente, C., Olague, G., Smith, S.V., Bullock, S.H., Hinojosa-Corona, A. and González-Botello, M.A. (2011) A genetic programming approach to estimate vegetation cover in the context of soil erosion assessment. *Photogrammetric Engineering and Remote Sensing,* 77(4): 363–376. https://doi.org/10.14358/PERS.77.4.363.

Renard, K.G. and Foster, G.R. (1983) Soil conservation: Principles of erosion by water. In

Dregne, H.E. and Willis, W.O. (eds.) *Dryland agriculture,* Agronomy Monograph, American Society of Agronomy, Madison: 155–176.

Renard, K.G. and Freimund, J.R. (1994) Using monthly precipitation data to estimate the R factor in the revised USLE, *Journal of Hydrology,* 157: 287–306.

Renard, K.G., Foster, G.R., Weesies, G.A., McCool, D.K. and Yoder, D.C. (1997) *Predicting soil erosion by water: a guide to conservation planning with the revised universal soil loss equation (RUSLE)*. Agriculture Handbook No. 703, USDA, Washington DC: 64p.

Renard, K.G., Yoder, D.C., Lightle, D.T. and Dabney, S.M. (2011) Universal soil loss equation and revised universal soil loss equation. In Morgan, R.P.C. and Nearing, M.A. (eds.), *Handbook of erosion modelling,* Blackwell Publishing Ltd., Chichester: 137–167.

Roy, S., Das, S., Sengupta, S., Mistry, S., Chatterjee, J. (2022) Monitoring the temporal dimension of soil erosion in Mayurakshi Basin, India: A novel approach integrating RUSLE, Shannon's entropy and landscape ecological metrics. *Journal of Earth System Science,* 131, 249: PP. http://doi.org/10.1007/s12040-022-02006-9.

Roy, S., Sengupta, S. (2019) Channel shifting and associated sedimentological characteristics of the Katwa-Mayapur stretch of the Bhagirathi-Hooghly river, Eastern India. *International Journal of Current Research,* 11: 3467–3473. https://doi.org/10.24941/ijcr.35131.04.2019.

Setegn, S.G., Dargahi, B., Srinivasan, R., Melesse, A.M. (2010) Modeling of sediment yield from Anjeni-Gauged Watershed, Ethiopia using SWAT model. *Journal of the American Water Resources Association,* 46(3): 514–526. http://doi.org/10.1111/j.1752-1688.2010.00431.x.

Sharda, V.N., Mandal, D., Ojasvi, P.R. (2013) Identification of soil erosion risk a reas for conservation planning in different states of India. *Journal of Environmental Biology,* 34 (2): 219–226.

Sheikh, A.H., Palria, S. and Alam, A. (2011) Integration of GIS and Universal Soil Los Equation (USLE) for soil loss estimation in a Himalayan Watershed, 3, pp: 51–57.

Toy, T.J., Foster, G.R., Renard, K.G. (1999) RUSLE for mining, construction and reclamation lands. *Journal of Soil and Water Conservation,* 54(2): 462–467.

Uddin, K., Murthy, M.S.R., Wahid, S.M., Matin, M.A. (2016) Estimation of soil erosion dynamics in the Koshi basin using GIS and remote sensing to assess priority areas for conservation. *PLoS One,* 11(13): 1–19. http://doi.org/10.1371/journal.pone.0150494.

Van der Knijff, J.M., Jones, R.J.A., Montanarella, L. (2000) Soil erosion risk assessment in Italy. European Soil Bureau, Joint Research Centre of the European Commission. http://eusoils.jrc.ec.europa.eu/ESDB_Archive/pe sera/pesera_cd/ pdf/ ereurnew2.pdf (retrieved on 2024-02-01).

Van Remortel, R.D., Hamilton, M.E., Hickey, R.J. (2001) Estimating the LS factor for RUSLE through iterative slope length processing of digital elevation data within Arclnfo grid. *Cartography,* 30(1): 27–35.

Vijith, H., Seling, L.W., Dodge-Wan, D. (2017) Effect of cover management factor in quantification of soil loss: Case study of Sungai Akah sub-watershed, Baram river basin Sarawak, Malaysia. *Geocarto International,* 33(5): 1–17. http://doi.org/10.1080/10106049.2016.1273398.

Wang, G., Wente, S., Gertner, G. Z., Anderson, A. (2002) Improvement in mapping vegetation cover factor for the universal soil loss equation by geostatistical methods with Landsat Thematic Mapper images. *International Journal of Remote Sensing,* 23(18): 3649–3667. http://doi.org/10.1080/01431160110114538.

Wischmeier, W.H., Smith, D.D. (1978) *Predicting rainfall erosion losses: a guide to conservation planning.* Agriculture Handbook No. 537, USDA, Washington, DC: 69p.

Yue-Qing, X., Jian, P. Xiao-mei, S. (2009) Assessment of soil erosion using RUSLE and GIS: a case study of the Maotiao River watershed, Guizhou Province, China. *Environmental Geology,* 56: 1643–1652.

Yuksel, A., Gundogan, R., Akay, A.E. (2008) Using the remote sensing and GIS technology for erosion risk Mapping of Kartalkaya Dam Watershed in Kahramanmaras, Turkey. *Sensors,* 8: 4851–4865.

Zhang, H., Yang, Q., Li, R., Liu, Q., Moore, D., He, P., Geissen, V. (2013) Extension of a GIS procedure for calculating the RUSLE equation LS factor. *Computers and Geosciences,* 52: 177–188. http://doi.org/10.1016/j.cageo.2012.09.027.

Zhu, L., Zhang, H., Guo, L., Huang, W. and Gong, W. (2021) Estimation of riverine sediment fate and transport timescales in a wide estuary with multiple sources. *Journal of Marine Systems,* 214(103488): 1–14. http://doi.org/10.1016/j.marsys.2020.103488.

Date received: 17 March 2024
Date accepted after revision: 31 October 2024